Local arrangement of silylene groups on Si(100)2×1 after SiH_4 decomposition

J. Spitzmüller, M. Fehrenbacher, M. Pitter, H. Rauscher,* and R. J. Behm*
Abteilung Oberflächenchemie und Katalyse, Universität Ulm, D-89069 Ulm, Germany
(Received 8 August 1996)

The interaction between Si(100)2×1 and SiH_4 under UHV chemical vapor deposition conditions between 550 and 690 K is studied with high-resolution scanning tunneling microscopy and kinetic model calculations. In addition to small anisotropic Si islands and patches of hydrogen-terminated substrate, metastable cross-shaped structural tetramer units are formed in this temperature region. These tetramers are interpreted as a combination of four SiH_2 groups connecting four Si substrate atoms, and their coverage is correlated with the decomposition kinetics of SiH_2. [S0163-1829(97)05707-X]

I. INTRODUCTION

The decomposition of SiH_4 on Si(100) is one of the most important reactions on semiconductor surfaces because of its use in Si thin-film epitaxial growth by chemical vapor deposition (CVD). Hence a detailed knowledge of the contributing processes, on an atomic scale, is desirable to find the optimum process parameters for Si deposition. So far this reaction has been investigated mainly with spatially averaging methods like temperature-programmed desorption (TPD),[1,2] static secondary-ion mass spectroscopy (SSIMS),[1] and time-of-flight mass spectroscopy (TOF-MS).[3] Based on these investigations a reaction scheme was set up.[1] A detailed understanding of the decomposition and Si forming process and of the various intermediate species, however, was hampered by the lack of topographic information. We therefore started an extensive scanning tunneling microscopy (STM) study on Si epitaxy by decomposition of SiH_4 on Si(100)2×1. Results concerning the Si island growth behavior and the diffusion of intermediate species were published recently.[4,5] In this work we report on a metastable surface species observed after deposition in the temperature range 550–690 K. From our STM measurements, kinetic model calculations, and by drawing on earlier work on SiH_4 decomposition on Si(100)2×1, this species is identified as a tetramer consisting of four SiH_2 groups.

II. EXPERIMENT

The experiments were performed in a STM-equipped UHV system described elsewhere.[6] The samples were cut from commercial *p*-Si(100) wafers with a resistivity of 0.025 Ω cm and a miscut of 0.3°, and cleaned using standard procedures. They can be heated in a heating stage, by electron impact from the back, to temperatures up to 1500 K. Monosilane is introduced into the chamber through a precision leak valve. After checking the surface for cleanliness and low defect concentration, the sample is exposed to SiH_4 (typically 10^{-7}–10^{-5} mbar partial pressure, 2% silane in Ar) at a selected substrate temperature. After the exposition the sample is cooled down to room temperature, and then transferred to the tunneling stage. Images are typically recorded with a tunneling current of ~30 pA and a sample voltage of −1.7 V. Darker tones in the images correspond to lower areas in the topography [with the exception of Fig. 4(a)].

III. RESULTS AND DISCUSSION

Adsorption of SiH_4 was carried out on clean and well-prepared Si(100)2×1 samples, which show the well-known dimer reconstruction with a low defect concentration of a few percent. Typical surface structures which can be observed on these surfaces after SiH_4 decomposition between 550 and 690 K are illustrated in Fig. 1. This figure shows a STM image of a surface area with two terraces separated by an S_B step (i.e., the dimer rows of the upper terrace are perpendicular to the step edge), after exposure to 340-L SiH_4 at 690-K substrate temperature and a pressure $p(SiH_4)=1\times10^{-5}$ mbar. The image resolves the 2×1 reconstruction of the surface with dimer rows rotated by 90° relative to each other on subsequent terrace levels. Si islands grown by SiH_4 decomposition at this temperature and coverage (0.1 ML) are anisotropic;[4,5] their preferential growth direction is perpendicular to the underlying Si dimer rows. Both isolated dimers as well as dimer strings one dimer wide and several dimers long are found in the image, in addition to some wider islands. Adsorbed hydrogen atoms resulting from SiH_4 dissociation are paired on the substrate dimer units, whereas the islands are free of hydrogen.[4] Both adsorbed hydrogen and vacancies appear as darkened Si sites in the images presented here, as described previously,[5,7] but the hydrogen-terminated dimers can still be detected under appropriate conditions, such as in Fig. 1, and can therefore be distinguished from missing dimer units.[7] In this temperature regime, besides the SiH_x species ($x=2$ and 3), the hydrogen adatoms are also mobile[8] and form patches of aggregated adsorbed hydrogen islands,[7] indicating that there is a net attractive H-H interaction.

In addition to Si islands and hydrogen-terminated Si areas already reported in earlier work,[5] an interesting surface species (see, e.g., arrows in Fig. 1) is observed after deposition under these conditions. These structures are cross shaped and have similarities with four-leaf clovers. They are termed ''cloverleaf structures'' in the following. At 690-K growth temperature only a few of these structures are present (see Fig. 1), but they are observed in the entire temperature regime examined, from 550 to 690 K, with different tunneling

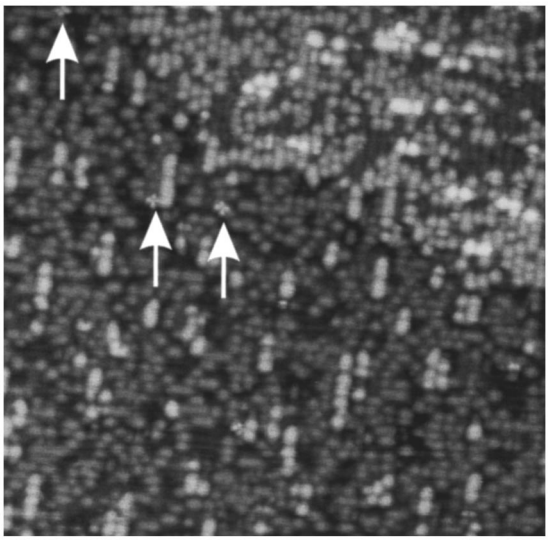

FIG. 1. STM image (480×480 Å^2) of the Si(100) surface after exposure to 340-L SiH_4 [$p(SiH_4)=1\times10^{-5}$ mbar, 2% in Ar] at 690-K substrate temperature. Beside this, anisotropic Si islands and patches of aggregated adsorbed hydrogen cross-shaped (''cloverleaf'') structures (indicated by arrows) can be seen. Sample voltage: −1.7 V; tunnel current: 40 pA.

tips, in different experiments and with different Si samples. The density of the cloverleaf structures depends strongly on the deposition conditions, i.e., substrate temperature and SiH_4 flux. The lower the substrate temperature (between 550 and 690 K), the more of these species are observed. A large number of them can be identified in Fig. 2, after 340-L exposure at a substrate temperature of 570 K and $p(SiH_4)=2\times10^{-6}$ mbar. This image shows a surface area with two terraces separated by a monoatomic step running from the upper left to the lower right. Even here, at a temperature as low as 570 K, small 2×1 islands are formed,

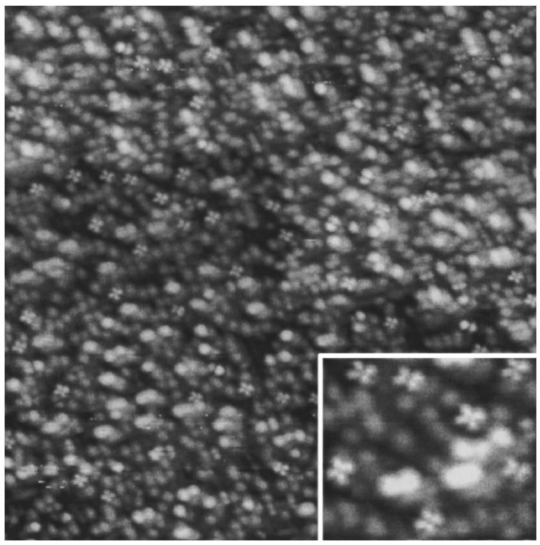

FIG. 2. STM image (420×420 Å^2) of the Si(100) surface after exposure to 340-L SiH_4 [$p(SiH_4)=2\times10^{-6}$ mbar] at 570-K substrate temperature. The density of the clover structures is much higher than in Fig. 1. The inset shows an enlarged detail of the image. Sample voltage: −1.7 V; tunnel current: 30 pA.

consisting of 1–4 dimers. The shape of the two-dimensional islands is less anisotropic, and the island density is increased compared to Si growth at 690 K (see Fig. 1), which can be among others attributed to a reduced mobility of the Si or SiH_x species.

At this growth temperature a concentration of 2.3×10^{12} cm^{-2} is found for the cloverleaf structures after exposure to 340-L SiH_4. Their distribution on the surface is homogeneous, and we did not detect any preferential sites such as step edges. The structures are fourfold symmetric, with four clear maxima. The height of the maxima extends about 0.7 Å above the surrounding silicon substrate dimer units under these tunneling conditions. When exposing the surface at room temperature to SiH_4, we did not detect any of these symmetric features. Also, above 690-K substrate temperature none of these cloverleaf structures are found. However, once they are formed, these structures are stable at least on a time scale of hours after quenching the sample to room temperature. However, after tempering the sample at 850 K, these structures disappear.

To gain further information about the nature of the cloverleaf structures, we consider the reaction scheme proposed in Refs. 1 and 9 for SiH_4 decomposition on Si(100)2×1. It includes the following steps:

$$SiH_4(g)+2\,db\rightarrow\underline{H}+\underline{SiH_3}, \tag{1}$$

$$\underline{SiH_3}+2\,db\rightarrow\underline{H}+\underline{\underline{SiH_2}}, \tag{2}$$

$$2\,\underline{\underline{SiH_2}}\rightarrow H_2(g)+H-\underline{\underline{Si}}-\underline{\underline{Si}}-H, \tag{3}$$

and/or

$$2\,\underline{\underline{SiH_2}}+2\,db\rightarrow2\underline{H}+H-\underline{\underline{Si}}-\underline{\underline{Si}}-H, \tag{4}$$

$$H-\underline{\underline{Si}}-\underline{\underline{Si}}-H\rightarrow H_2(g)+\underline{\underline{Si}}=\underline{\underline{Si}}, \tag{5}$$

$$2\underline{H}\rightarrow H_2(g)+2\,db. \tag{6}$$

The symbol db is used for a dangling bond of a Si surface atom, and the number of surface bonds of a Si or H atom is indicated by single and double underlining, respectively. SiH_4 reacts at with two db's on one dimer or with two db's on adjacent dimers within a row dissociatively under formation of adsorbed hydrogen and adsorbed SiH_3 groups [Eq. (1)]. SiH_3 was found to dissociate at temperatures below 600 K under saturation of free db's of the surface following reaction (2),[1] without H_2 desorption into the gas phase. The next dissociation product, SiH_2, is stable at room temperature.[10] The decomposition mechanism of SiH_2 depends on the initial SiH_3 coverage. At higher coverages (≥0.02 ML), where the surrounding db sites are saturated either by adsorbed SiH_x or H species, SiH_2 dissociates between 675 and 775 K, producing desorbing hydrogen (β_2 peak in TPD),[1] and the monohydride [Eq. (3)]. At low initial SiH_3 coverages (0.02 ML), SiH_2 dissociates between 600 and 750 K, under formation of adsorbed hydrogen and SiH [Eq. (4)]. Here the hydrogen atoms can adsorb on neighboring db sites. Isolated SiH is either short lived as an isolated species, or it dimerizes under formation of a hydrogen-terminated Si dimer. Finally, hydrogen desorption from the monohydrides [Eqs. (5) and (6)] occurs above about 700 K (β_1 peak in TPD).[1] To analyze the stability range of the SiH_4 dissociation products and their concentration in different temperature

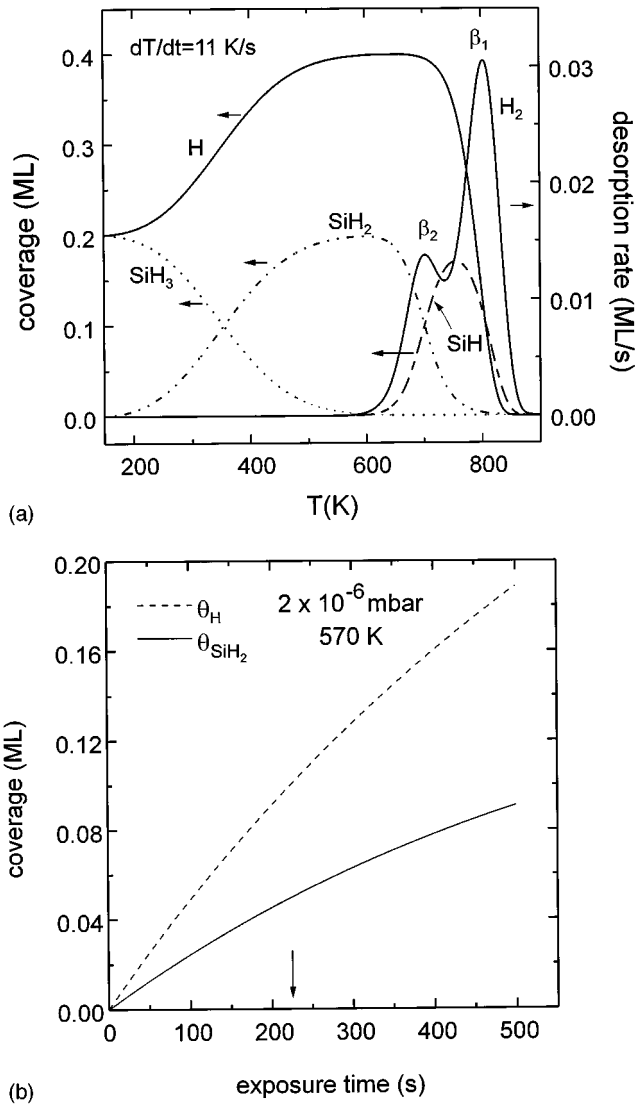

FIG. 3. (a) Calculated thermal evolution of the SiH_4 dissociation products SiH_3, SiH_2, SiH, H, and desorbing H_2 upon annealing (11 K/s), after adsorption of 0.2-ML SiH_4 on Si(100)2×1 at 150 K. The parameters (activation energies for dissociation/desorption, preexponentials) are taken from Refs. 1, 11, and 12. (b) Calculated temporal evolution of the SiH_2 and H coverages upon exposure of Si(100)2×1 to SiH_4 [570 K, $p(SiH_4)=2\times10^{-6}$ mbar]. The SiH and SiH_3 coverages are completely negligible under these conditions. The SiH coverage becomes important only far beyond the displayed exposure time by decomposition of SiH_2. The arrow indicates the exposure after which the image in Fig. 2 was recorded.

regimes, in particular in the regime where cloverleaf structures are observed, we performed numerical simulations on the coupled SiH_4 dissociation cascade [Eqs. (1), (2), (3), (5), and (6)] using values for the reaction rate constants from Refs. 1, 11, and 12 (see the Appendix). Since no information is available for the kinetics of Eq. (4), this channel for SiH_2 dissociation was not considered. Results of these calculations are shown in Fig. 3. The first graph [Fig. 3(a)] illustrates the evolution of the different SiH_4 dissociation species after adsorption of SiH_4 at 150 K and subsequent heating of the surface. The parameters (adsorption temperature 150 K, initial coverages of SiH_3 and H 0.2 ML for each species, heating rate 11 K/s) are the same as in the experiments of Ref. 1. When comparing the results of the measurements in Ref. 1 with our simulations, there is excellent agreement as far as the evolution of SiH_3 and desorption of H_2 (β_2 and β_1 peaks) are concerned. The calculations show that SiH_2 is by far the most abundant SiH_x species between 500 and 700 K, whereas most of the SiH_3 is dissociated up to 500 K. Only above 700 K is the SiH coverage larger than the SiH_2 coverage in a narrow temperature regime.

Results for the temporal evolution of the H and SiH_2 coverage during SiH_4 exposure (2×10^{-6} mbar), at a temperature of 570 K, are shown in Fig. 3(b). While SiH_2 is the majority species under these conditions, the SiH_3 and SiH coverages are clearly negligible. After 225 s of SiH_4 dosing [i.e., 340 L; see the arrow in Fig. 3(b)] steady-state conditions are not yet reached. The corresponding surface topography resulting after such an exposure is displayed in the STM image of Fig. 2. At this point the SiH_2 coverage is about 4% of a monolayer, while the deposited amount of Si is ~0.07 ML and the db concentration is 85%.

Since in our experiments the SiH_4 exposure was carried out between 550 and 690 K, we expect the majority of the SiH_x species to be SiH_2. It is therefore very reasonable to propose that the SiH_2 groups play a major role in the formation of the cloverleaf structures. To confirm this, we consider the possible dissociation fragments SiH_3, SiH_2, and adsorbed H from monosilane molecules, and their bonding geometries on Si(100)2×1.

In order to achieve fourfold tetrahedral coordination for the Si atom, a SiH_3 group would be bonded directly to one of the terminal dangling bonds of a Si═Si dimer. An isolated adsorbed SiH_2 group is located midway between two dimers of the same dimer row, in an off-center position, with the underlying dimer σ bond intact, as reported for Si_2H_6 dissociation.[10] As identified in previous experiments on disilane adsorption and dissociation, which produces the same surface species as monosilane,[1] a SiH_3 group would appear as a protrusion at negative sample bias, whereas adsorbed hydrogen can be identified as darkened Si sites.[13] Such protruding SiH_3 structures are, however, not observed, and are also not expected in the temperature regime investigated, because these species dissociate too fast. Indeed, after Si_2H_6 adsorption, SiH_3 already decomposes within a few minutes at 300 K, while isolated SiH_2 groups can be observed up to 540 K.[13] Therefore, and because of the simulation results described above, we suggest that the four-leaf clover is formed by a combination of four SiH_2 groups. Individual Si dimers, on the other hand, which at a first sight also seemed to be conceivable as tetramer building units, appear larger in width and height than the four maxima in the cloverleaf structure under these tunnel conditions, which can also be seen by direct comparison with individual dimers in Fig. 2. They can therefore be excluded as clover building units.

Details of the bonding geometry of the cloverleaf structures can be derived from a close-up of the silane-dosed surface, where one such feature can be seen [Fig. 4(a)]. We would like to note here that it is very difficult to obtain atomic resolution for both cloverleaf structures and the substrate. As a guide to the eye, grid lines parallel and perpendicular to the substrate dimer rows (midway between the rows and between neighboring dimers), are also drawn in

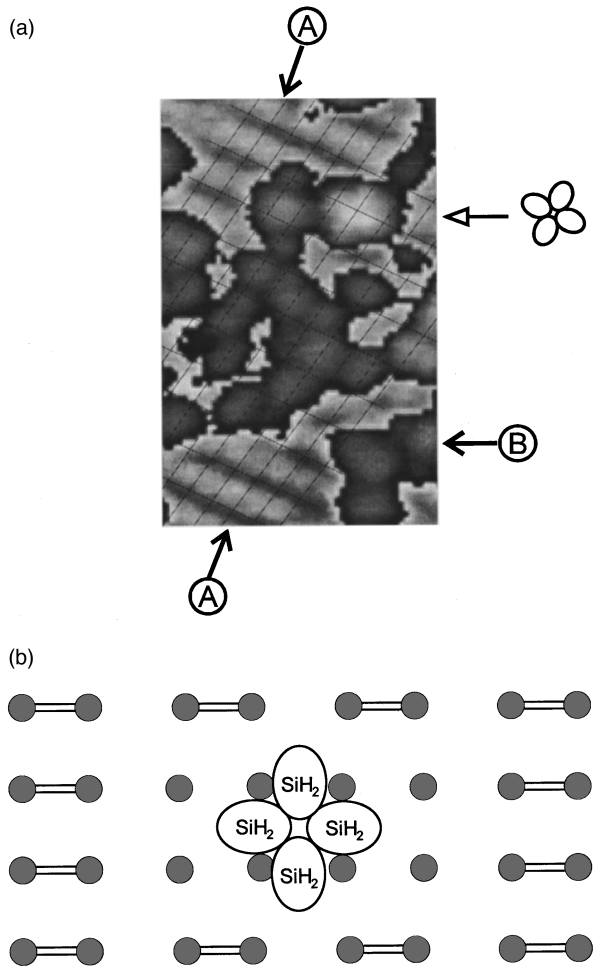

FIG. 4. (a) Enlarged detail (85×70 Å^2, SiH_4 deposition temperature 550 K) of a cloverleaf structure showing its bonding geometry on the surface; grid lines are drawn parallel and perpendicular to the substrate dimer rows, midway between the rows and between the Si dimers. Two different gray scales are used to enhance the contrast at the substrate and adsorbate level and to facilitate the determination of the exact position of the cloverleaf structure with respect to the dimers of the substrate. In this representation, hydrogen-free substrate dimers appear as cloudy structures. Image conditions as in Fig. 2. (b) Schematic illustration of the proposed tetramer structure with four SiH_2 groups.

this figure. In addition to the clover structure the surface contains H-terminated dimer rows [marked A in Fig. 4(a)] as well as clean 2×1 areas [marked B]. The former appear slightly lower in STM images. To enhance the contrast, we used two separate gray scales for these areas. Inspecting the clover species, we find that it is centered in the minimum between two neighboring dimer rows, with two maxima between the dimer rows and the other two each extending into one dimer row, centered between the dimers. The latter two maxima resemble the bonding geometry expected for two SiH_2 groups, which are each bridge bonded between two dimers within a single row, leaving the Si-Si dimer σ bond intact.[10] Such a configuration of paired SiH_2 groups was already seen after disilane dissociation as a precursor for silylene decomposition.[13]

The resulting model for a symmetric tetramer consisting of four SiH_2 groups is schematically sketched in Fig. 4(b). This structure implies that at the four substrate dimers involved both the weaker Si═Si π bonds as well as the stronger σ bonds are broken. As a result a local unreconstructed 1×1 surface with a surface Si-atom separation of 3.84 Å is produced. Each Si surface atom involved is bound to two SiH_2 groups, and each SiH_2 group forms two backbonds to adjacent substrate atoms. This way every silicon atom in the adsorption complex (four Si atoms from SiH_2 groups and four substrate Si atoms) is fourfold coordinated. In this model, the four Si atoms of the SiH_2 groups can adopt an almost ideal tetrahedral configuration. The bonds of the four involved substrate atoms are strained, since two of the SiH_2 groups are shifted from the ideal tetraeder positions, while the Si atoms of the other two silylene groups can be bonded at bulklike positions, but probably all bonds in the adsorption complex will be relaxed to a certain degree as compared to the bulk bond lengths and angles. Hence the clover structure can be built up by four SiH_2 groups by a modification of the Si tetrahedral bonding geometry with moderate strain. In this tetramer bonding model, half of the broken substrate dimer atoms are not involved in its basic configuration. Since this is energetically unfavorable, several secondary processes are conceivable, such as termination of their db's with hydrogen or Si═Si dimerization (in the direction perpendicular to the original dimers) or a combination of these processes. This question, however, cannot be answered from the present data. The energetically unfavorable process of breaking the strong Si—Si σ bond, which might appear as an argument against the above interpretation, is also necessary for formation of epitaxial 2×1 islands and occurs at this temperature of 550–570 K [Figs. 2 and 4(a)], and in molecular-beam epitaxy even at room temperature.[14]

Since in bulk silicon the Si—Si bond length is 2.35 Å, the surface Si atom separation on the unreconstructed, ideally bulk-terminated Si(100) surface would be 3.84 Å because of the tetrahedral bonding angle of 109.5°. The arrangement of four SiH_2 groups as described above is the sterically most reasonable configuration for the four-leaf clover, as observed with STM. A SiH_2 group bridging two unreconstructed surface Si atoms with tetrahedral geometry would have Si—Si bond lengths close to that of bulk silicon, because in this configuration the relative positions of six Si atoms (two SiH_2 and four substrate atoms) involved in bonding are nearly the same as in the bulk. This holds for the two Si atoms of the SiH_2 groups which are in a plane with the substrate atoms underneath which is parallel to the dimer orientation, while the other two SiH_2 groups are shifted from the bulklike positions. We therefore propose that the feature shown in Fig. 4 is an arrangement of four SiH_2 groups, bound to the surface in the geometry discussed above.

Similar features were not found in previous experiments on interaction of disilane with Si(100)2×1 at room temperature or subsequent annealing.[10,13] We mainly relate this to the different experimental conditions in Refs. 10 and 13. Those experiments were performed by dosing the surface with disilane at room temperature (RT), subsequent annealing to various temperatures, and imaging with the STM after quenching the sample to RT. Isolated, randomly adsorbed SiH_2 groups from dissociated Si_2H_6 were identified, which disappeared after annealing to temperatures above 540 K. In contrast, we exposed the surface continuously with monosi-

lane between 550 and 690 K, and imaged the result with the STM after quenching the sample to RT. Under deposition conditions a steady concentration of mobile SiH_2 groups emerging from SiH_3 decomposition exists, which facilitates nucleation of the tetramers by aggregation of SiH_2 species. From the values reported for the diffusion barrier of Si (Ref. 15) (1.44 eV) or SiH_x (Ref. 5) (1.24 eV) in the presence of coadsorbed, mobile hydrogen the mobility of SiH_2 in the investigated temperature regime should be high enough that individual SiH_2 groups can meet and nucleate tetramer units before they dissociate. We expect that these tetramer structures can also be formed by Si_2H_6 decomposition, provided the exposure is carried out at appropriate temperatures.

Finally, we want to briefly discuss the energetics of the tetramer structures. For the latter ones, four Si═Si dimer σ bonds and four dimer π bonds have to be broken, while for four individual SiH_2 groups breaking of eight dimer π bonds is necessary. This would clearly favor the individual SiH_2 species. If we allow the four Si atoms aside the tetramer units to dimerize, they could additionally form two σ and two π bonds. This should still be less favorable than four individual SiH_2 species, but the tetramers might be stabilized by strain energy released during their formation. The stable final structures of course are Si islands.

IV. SUMMARY

In summary we have shown that during adsorption of SiH_4 on Si(100)2×1 between 550 and 690 K, and thermal decomposition beside normal Si island growth, a metastable species (''cloverleaf structure'') can be formed. This species is identified as a SiH_2-tetramer configuration which probably nucleates by coalescence of SiH_2 groups, the majority SiH_x species in this temperature regime.

ACKNOWLEDGMENTS

This work was supported by the Stiftung Volkswagenwerk under Grant No. I/67727. The Si samples were kindly provided by Wacker Chemitronic.

APPENDIX

The stoichiometric reaction scheme leading to Si film growth from SiH_4 decomposition can be described in the following manner:[9]

$$2\,SiH_4(g) + 4\,db \xrightarrow{k_1} 2\underline{H} + 2\underline{Si}H_3,$$

$$2\underline{Si}H_3 + 2db \xrightarrow{k_2} 2\underline{H} + 2\underline{\underline{Si}}H_2,$$

$$2\underline{\underline{Si}}H_2 \xrightarrow{k_3} H_2(g) + H-\underline{\underline{Si}}-\underline{\underline{Si}}-H,$$

$$H-\underline{\underline{Si}}-\underline{\underline{Si}}-H \xrightarrow{k_4} H_2(g) + 2db + \underline{\underline{Si}}=\underline{\underline{Si}},$$

$$4\underline{H} \xrightarrow{k_4} 2H_2(g) + 4db.$$

The reaction constant k_l is defined as $k_1 = k_1^0 \times \exp[-E_a/(R\times T)]$, with an activation energy E_a of 3 kcal/mole for SiH_4 adsorption,[9] and the preexponential k_1^0 is calculated from the relation $S_R = 2\times N_{Si}^2 \times k_1^0 \times \exp[-E_a/(R\times 673\ \mathrm{K})]$,[9] using a sticking probability of SiH_4 on Si(100) of $S_R = 5\times 10^{-4}$ which is derived from growth rate measurements.[4] N_{Si} is the density of dangling bonds on the Si(100) 2×1 surface (6.8×10^{14} cm^{-2}). The decomposition of SiH_3 groups is assumed to be pseudo-first-order, with an activation energy of 2 kcal/mole and a preexponential of $k_2^0 = 0.85\ \mathrm{s}^{-1}$.[1] The decomposition of silylene groups is second order with an activation energy of 43 kcal/mole and a preexponential of $k_3^0 = 4.7\times 10^{-2}\ \mathrm{cm}^2\ \mathrm{s}^{-1}$.[11] The desorption of H_2 from the Si monohydride state is first order, with an activation energy of 47 kcal/mole and a preexponential of $k_4^0 = 8\times 10^{11}\ \mathrm{s}^{-1}$.[12] The time evolution of the coverages for the individual species was then derived from the following scheme of coupled differential equations:

$$\frac{d\theta_{\underline{SiH_3}}}{dt} = 2\times k_1 \times p_{SiH_4} \times \theta_{db}^2 - 2\times k_2 \times \theta_{\underline{SiH_3}},$$

$$\frac{d\theta_{\underline{\underline{SiH_2}}}}{dt} = 2\times k_2 \times \theta_{\underline{SiH_3}} - 2\times k_3 \times \theta_{\underline{\underline{SiH_2}}}^2,$$

$$\frac{d\theta_{\underline{\underline{SiH}}}}{dt} = 2\times k_3 \times \theta_{\underline{\underline{SiH_2}}}^2 - 2\times k_4 \times \theta_{\underline{\underline{SiH}}},$$

$$\frac{d\theta_H}{dt} = 2\times k_1 \times p_{SiH_4} \times \theta_{db}^2 + 2\times k_2 \times \theta_{\underline{SiH_3}} - 4\times k_4 \times \theta_{\underline{H}},$$

$$\frac{d\theta_{db}}{dt} = 2\times k_4 \times \theta_{\underline{\underline{SiH}}} + 4\times k_4 \times \theta_{\underline{H}} - 4\times k_1 \times p_{SiH_4} \times \theta_{db}^2 - 2\times k_2 \times \theta_{\underline{SiH_3}},$$

with the condition $\theta_{\underline{SiH_3}} + \theta_{\underline{\underline{SiH_2}}} + \theta_{\underline{\underline{SiH}}} + \theta_{db} = N_{Si}$.
These five coupled differential equations were solved by numerical integration using Euler's method with a time increment of 10^{-4} s.

*Electronic address: hubert.rauscher,juergen.behm@chemie.uni-ulm.de

[1] S. M. Gates, C. M. Greenlief, and D. B. Beach, J. Chem. Phys. **93**, 7493 (1990).
[2] F. Hirose, M. Suemitsu, and N. Miyamoto, J. Appl. Phys. **70**, 5380 (1991).
[3] S. M. Gates and S. K. Kulkarni, Appl. Phys. Lett. **60**, 53 (1992).
[4] M. Fehrenbacher, J. Spitzmüller, U. Memmert, H. Rauscher, and R. J. Behm, J. Vac. Sci. Technol. A **14**, 1499 (1996).
[5] J. Spitzmüller, M. Fehrenbacher, H. Rauscher, and R. J. Behm (unpublished).
[6] F. Donig, A. Feltz, M. Kulakov, H. E. Hessel, U. Memmert, and R. J. Behm, J. Vac. Sci. Technol. B **11**, 1955 (1993).
[7] J. J. Boland, J. Vac. Sci. Technol. A **10**, 2458 (1992).
[8] D. A. Hansen, M. R. Halbach, and E. G. Seebauer, J. Chem. Phys. **104**, 7338 (1996).

[9] S. M. Gates and S. K. Kulkarni, Appl. Phys. Lett. **58**, 2963 (1991).
[10] M. J. Bronikowski, Y. Wang, M. T. McEllistrem, D. Chen, and R. J. Hamers, Surf. Sci. **298**, 50 (1993).
[11] P. Gupta, V. L. Colvin, and S. M. George, Phys. Rev. B **37**, 8234 (1988).
[12] K. Sinniah, M. G. Sherman, L. B. Lewis, W. H. Weinberg, J. T. Yates, Jr., and K. C. Janda, Phys. Rev. Lett. **62**, 567 (1989).
[13] Y. Wang, M. J. Bronikowski, and R. J. Hamers, Surf. Sci. **311**, 64 (1994).
[14] Y.-W. Mo, J. Kleiner, M. B. Webb, and M. G. Lagally, Surf. Sci. **268**, 275 (1992).
[15] J. E. Vasek, Z. Zhang, C. T. Salling, and M. G. Lagally, Phys. Rev. B **51**, 17 207 (1995).